Journal of Catalysis **211,** 198–207 (2002)
doi:10.1006/jcat.2002.3697

Siting and Distribution of the Co Ions in Beta Zeolite: A UV–Vis–NIR and FTIR Study

J. Dědeček, L. Čapek, D. Kaucký, Z. Sobalík, and B. Wichterlová[1]

J. Heyrovský Institute of Physical Chemistry, Academy of Sciences of the Czech Republic, Dolejškova 3, CZ-182 23 Prague 8, Czech Republic

Received March 12, 2002; revised May 10, 2002; accepted May 10, 2002

The Co(II) ion sites in dehydrated beta zeolites, consisting of polymorphs A, B, and C, were identified using an approach based on a similarity between visible spectra of the Co(II) ions in mordenite, ferrierite ZSM-5, and beta zeolites, and similarity in local framework structures accommodating the Co(II) ions in these zeolites. The results were supported by FTIR spectra in the region of skeletal vibrations showing the characteristic shifts of framework T–O–T vibrations induced by the framework perturbations due to the Co(II) ions at cationic sites. Three different cationic sites accommodating divalent metal ions in beta zeolite were found. Their positions in the channel system and local framework arrangements in different polymorphs of beta zeolites were suggested. The α-site is formed in polymorph C of the beta structure by an elongated six-member ring composed of twofold connected five-member rings. The Co(II) ions at the α-site exhibit an absorption band at 14,600 cm^{-1} in the visible spectrum and a band at 901 cm^{-1} in the IR spectra. The β-site present in polymorphs A and B is formed by a planar deformed six-member ring of the hexagonal cage. The Co(II) ions at the β-site are characterized by four bands, at 15,500, 16,300, 17,570, and 21,700 cm^{-1} in the visible spectrum and by a band at 918 cm^{-1} in IR spectra. The γ-site occurring in polymorphs A and B of the beta structure is located inside the hexagonal cage. The Co ions at the γ-site are reflected in a doublet, at 18,500 and 20,100 cm^{-1} in the visible spectra.

Key Words: **Co–beta; Co(II) ions; cation siting; visible spectroscopy; FTIR.**

INTRODUCTION

Co ions exchanged in beta zeolite have been shown to exhibit exceptional catalytic activity among cobalt pentasil ring zeolites, as Co–ZSM-5, Co–ferrierite, and Co–mordenite. The Co–beta zeolites possess high and stable activity in selective catalytic reduction of NO (SCR-NO$_x$) with propane in a high excess of water vapor (1, 2), as exists in real exhaust gases of combustion processes, and in ethane ammoxidation to acetonitrile (3, 4). However, the structure of the active site in this zeolite remains unknown, although there are clear indications on the presence of various Co ion types in Co–beta zeolites (5, 6). Due to a low concentration of transition metal ions in zeolites of beta topology, a large unit cell and, moreover, three known beta polymorphs (A, B, and C), the identification of the cationic sites in beta zeolites from the XRD experiments, as for other pentasil ring zeolites, is difficult.

UV–vis–NIR diffuse reflectance spectra of Co(II) ions and FTIR spectra of perturbed skeletal T–O bonds due to Co(II) ion bonding at different cationic sites have been recently successfully used for the identification of the siting and distribution of the exchanged Co(II) ions in Co–ferrierite and Co–ZSM-5 (7–9). The suggestions regarding the Co ion siting have been based on the similarity of the Co(II) visible spectra and of the local framework structures hosting the Co ions in mordenite (10), ferrierite (7), and ZSM-5 (8). Three different Co sites, denoted α, β, and γ, in mordenite, ferrierite, and ZSM-5 of very similar coordinations were indicated. Quantitative analysis of the Co(II) visible spectra of Co–zeolites yielded information on the distribution of the Co(II) ions among the individual cationic sites. Corresponding perturbations of the framework T–O bonds induced by the bonding of different Co ion types were reflected in the characteristic bands of the IR spectra of dehydrated Co–zeolites in the region of framework antisymmetric T–O–T vibrations (9, 11–13).

The above approach has been employed in this study to estimate Co siting in beta zeolites. It represents the first step in an attempt to analyze the structure of the Co ions in beta zeolite, and it opens a possibility of identifying the structure of exceptionally active Co ion species in beta zeolites. The study deals with the Co–beta zeolites prepared by Co ion exchange at the condition that hydrolysis of Co ions does not take place, and by using parent zeolites which were calcined after synthesis at various conditions, thus containing different concentrations of Brønsted and Lewis sites, such as is typical for H–beta zeolites. Four types of Co ion species have been observed in the Co–beta zeolites and their coordination and location in the beta structure, with consideration of the occurrence of A, B, and C polymorphs in the samples, have been suggested.

[1] To whom correspondence should be addressed. E-mail: wichterl@jh-inst.cas.cz.

0021-9517/02 $35.00

TABLE 1

Chemical Composition of Parent Beta Zeolites

Zeolite	Si/Al	SiO_2 (wt%)	Al_2O_3 (wt%)	Na_2O (wt%)	K_2O (wt%)	H_2O (wt%)	NH_4 (wt%)	Brønsted sites[a] (mmol/g)	Lewis sites[a] (mmol/g)
H–beta-I	12.7	92.7	6.2	0.0	0.0	1.1	—	0.13	0.52
HNa–beta-II	15.6	93.6	5.1	0.5	0.0	1.8	—	0.33	0.28
HNa–beta-III	22.3	95.0	3.6	0.8	0.2	0.4	—	0.25	0.18
NH_4–beta-IV	14.2	92.5	5.5	0.0	0.0	0.0	2.0	0.63	0.19

[a] Determined by quantitative analysis of IR spectra of adsorbed d_3-acetonitrile on dehydrated zeolite.

EXPERIMENTAL

Parent Zeolites

H–beta zeolite with Si/Al = 12.7 (H–Beta-I, PQ Corp.), two laboratory synthesized HNa–beta zeolites with Si/Al = 15.6 (HNa–beta-II) and 22.3 (HNa–beta-III), and NH_4–beta-IV with Si/Al = 14.2, the latter synthesized via an alkaline cation free procedure (beta-IV, Research Institute of Inorganic Chemistry, Inc., CZ), were used. HNa–beta-II and -III zeolites were synthesized according to the modified procedures of Rubin (14) using silica sol (TOSIL, Silchem, CZ), $NaAlO_2$ (Ridel-de-Haën), tetraethylammonium bromide as a templating agent (TEABr, Fluka), NH_4OH, and NaOH (LACHEMA, CZ). The molar composition of the reaction mixture $Na_2O : (NH_4)_2O : (TEA)_2O : SiO_2 : Al_2O_3 : H_2O$ was 2.74 : 11.02 : 4.32 : 29.06 : 1.00 : 605 for synthesis of HNa–beta-II, and 4.17 : 0.00 : 7.14 : 49.70 : 1.00 : 517 for synthesis of HNa–beta-III. The as-synthesized zeolites HNa–beta-II and -III were calcined in a stream of dry nitrogen at 723 K for 12 h followed by calcination in dry oxygen at 773 K for 12 h. The conditions of template removal from a commercial H–beta-I sample are not known. The beta-IV zeolite was calcined in a stream of dry ammonia at 693 K for 4 h, exchanged with Na^+ ions and calcined in an oxygen stream at 820 K to remove the rest of the template, and subsequently exchanged by NH_4^+ ions to obtain NH_4–beta-IV. This zeolite contained high concentrations of Brønsted sites, and only small amounts of Al–O framework bonds were perturbed and exhibited Lewis site character (Table 1, and see below).

The crystallinity and phase purity of the as-synthesized and calcined zeolites were checked by X-ray powder diffraction (Siemens D5005) and FTIR spectra of skeletal vibrations (Nicolet Magna 550). The size of crystallites (0.1–0.5 μm) was determined using a scanning electron microscope (SEM, Philips). Chemical composition of parent beta zeolites was determined by atomic absorption spectrometry after the zeolite samples dissolution; it is given in Table 1. The concentration of unperturbed bridging OH groups and concentration of Brønsted (perturbed and unperturbed bridging OH groups) and Lewis sites, given in Table 1, were determined by quantitative analysis of FTIR spectra of OH groups and C≡N vibrations of adsorbed d_3-acetonitrile on Brønsted and Lewis sites (see below).

Co–Beta Zeolites

Ion exchange with Co nitrate solution of the parent zeolites was carried out at RT and pH values for the suspension during the exchange ranging from 2.8 to 4.0. The Co–beta zeolite samples were thoroughly washed with distilled water and dried in air at RT. Chemical composition of Co–beta zeolites, determined by atomic absorption spectrometry after their dissolution, and the conditions of the Co ion exchange are given in Table 2.

UV–Vis–NIR Diffuse Reflectance Spectroscopy

Dehydration of Co–zeolites was carried out under a vacuum of 7×10^{-2} Pa in two steps: 370 K for 30 min and 770 K for 3 h. This procedure guaranteed that the Co ions did not coordinate water molecules or OH groups, as evidenced

TABLE 2

Chemical Composition and Conditions of Preparation of Co–Beta Zeolites

Parent zeolite	Co/Al	$Co(NO_3)_2$ concentration (mol/L)	Conditions of ion exchange solution/zeolite (ml/g)	Time (h) × repetition
H–beta-I	0.16	0.05	140	5
	0.25	0.05	140	24 × 3
HNa–beta-II	0.02	0.001	20	3
	0.04	0.0017	20	3
	0.08	0.0034	20	3
	0.09	0.006	17	3
	0.20	0.0037	33	3
	0.28	0.03	20	3
	0.35	0.08	33	3
	0.37	0.018	17	3
	0.42	0.10	67	24
	0.45	0.10	67	24
HNa–beta-III	0.03	0.001	17	3
	0.20	0.005	33	3
	0.42	0.10	33	24 × 3
NH_4–beta-IV	0.55	0.05	42	6

from the NIR region of the spectrum (for details, see Refs. (7, 8, 10, 15)). After dehydration, the sample was cooled to ambient temperature and transferred under vacuum into an optical cell 5 mm thick and sealed. UV–Vis–NIR spectra were measured using a Perkin–Elmer UV–Vis–NIR spectrometer Lambda 19 equipped with a diffuse reflectance attachment with an integrating sphere coated by $BaSO_4$. Diffuse reflectance (DR) spectra were recorded in a differential mode with a parent dehydrated zeolite as a reference. The absorption intensity was obtained from the Schuster–Kubelka–Munk equation $F(R_\infty) = (1 - R_\infty)^2/2R_\infty$, where R_∞ was the measured value of diffuse reflectance from a semiinfinite layer. The $F(R_\infty)$ value is proportional to the absorption coefficient and the concentration of Co ions. Details of the measurement are given elsewhere (7, 8, 10). Spectra were processed and evaluated by using the Microcal Origin 4.1 software (Microcal Software, Inc., U.S.).

FTIR Spectroscopy

IR spectra of parent beta and Co–beta samples were measured at RT after evacuation (10^{-3} Pa) at 750 K in a standard glass vacuum cell equipped with KBr windows and a carousel sample holder with six samples. Adsorption of d_3-acetonitrile was carried out at RT, followed by desorption at RT for 20 min (see Ref. (16). A FTIR spectrometer Nicolet Magna-550 with a MCT-B low-temperature detector was used. For a single spectrum, 200 scans at resolutions of 2 cm^{-1} were collected. Samples were used as self-supported pellets of about 5 and 10 $mg \cdot cm^{-2}$ thickness for measurements in the region of skeletal vibrations and of adsorbed d_3-acetonitrile, respectively. Spectra intensities were normalized on the sample 5.5 $mg \cdot cm^{-2}$ thick using the integral area of the zeolite skeletal bands in the region between 1750 and 2100 cm^{-1}. Concentrations of unperturbed bridging OH groups (IR band at 3610 cm^{-1}) and Brønsted sites (sum of the unperturbed and perturbed bridging OH groups, a band at 2297 cm^{-1} of C≡N vibrations of adsorbed d_3-acetonitrile) and Lewis sites (band at 2325 cm^{-1} of C≡N vibrations), determined by using extinction coefficients $\varepsilon_{OH} = 4.05 \pm 0.21$, $\varepsilon_B = 2.05 \pm 0.10$, and $\varepsilon_L = 3.62 \pm 0.16\ cm \cdot \mu mol^{-1}$, are given in Table 1. Determination of the extinction coefficients is given in Ref. (16) and details of the techniques are described in Refs. (11, 13). Positions and relative intensities of the bands in the "skeletal transmission window" (region between 950 and 880 cm^{-1}, where T–O–T skeletal vibrations were observed) were evaluated by a Fourier self-deconvolution procedure (OMNIC 4.1 software) of the spectra.

RESULTS

UV–Vis Spectra of Co–Beta Zeolites

The visible spectra of dehydrated Co–beta zeolites were similar to those reported for Co–mordenite, Co–ferrierite, and Co–ZSM-5 (cf. Refs. (7, 8, 10)). Normalized visible, spectra of dehydrated CoHNa–beta-II (Si/Al 15.6) and CoHNa–beta-III (Si/Al 22.3) possessing different Co/Al ratios are given in Fig. 1. A dependence of the integral intensity of the individual Gaussian bands on the chemical composition of Co–beta zeolites was employed for identification of the individual spectral components of the individual Co(II) ions. The decompositions of the spectra of Co–beta to the Gaussian bands of the spectral components α, β, and γ is illustrated in Fig. 2. Details of procedures are described in Refs. (7, 8, 10). Three types of "bare" Co(II) ions (coordinated exclusively to framework oxygens) were identified in Co–beta zeolites. The α-type Co(II) ions are represented by an absorption band at 14,600 cm^{-1}. The β-type Co(II) ions are characterized by a quartet, at 15,500, 16,300, 17,570, and 21,700 cm^{-1}, and a doublet, at 18,900 and 20,100 cm^{-1}, corresponds to the γ-type Co(II) ions. The ratios of the integral intensities of the individual bands of the spectral component β and γ being $0.2 \div 0.9 \div 1 \div 0.1$ and $1 \div 0.45$, respectively, confirmed their attribution to the corresponding components.

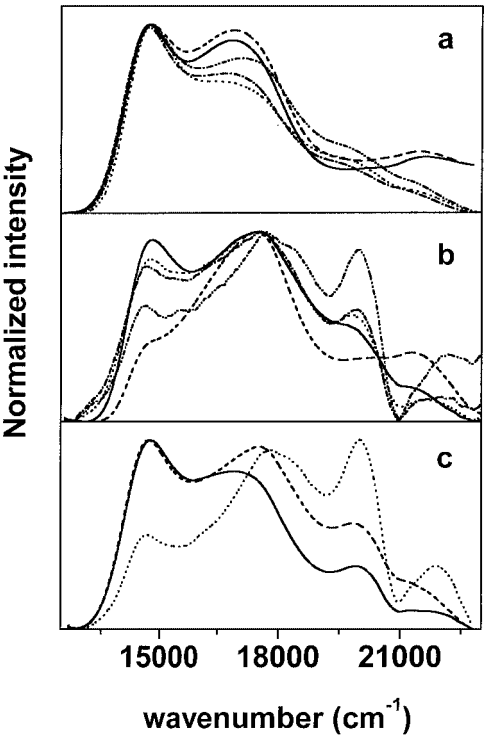

FIG. 1. Normalized visible spectra of CoHNa–beta-II zeolites: (a) Co/Al 0.45 (——), 0.42 (- - -), 0.37 (· · · ·), 0.35 (- · - · -), 0.28 (- · · ·); and (b) 0.20 (——), 0.09 (- - -), 0.08 (· · · ·), 0.04 (- · - · -), 0.02 (- · · ·). (c) CoHNa–beta-III zeolites: Co/Al 0.42 (——), 0.20 (- - - -), 0.03 (· · · ·).

The UV–vis spectrum of CoHNa–beta-II with Co/Al 0.36 and 0.45 is given in Fig. 3. An increase in Co loading above ca. Co/Al 0.35 was not followed by a significant increase in the intensity of d–d transitions, but by an increase in a new intensive band with maximum at ca. 31,500 cm^{-1}.

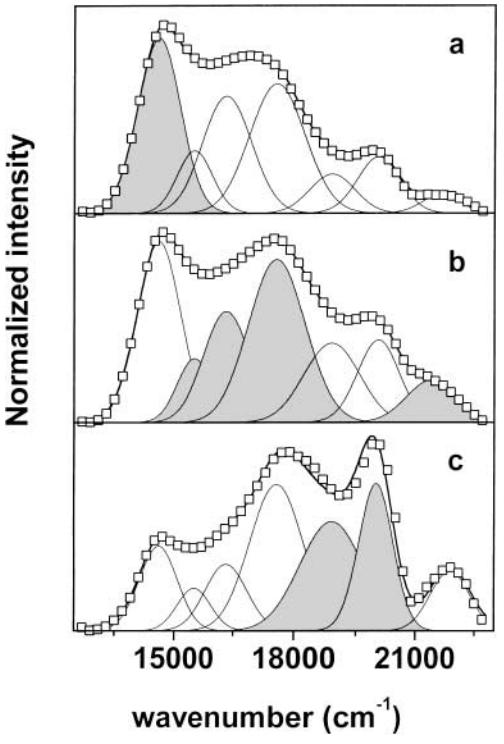

FIG. 2. Decomposition of the visible spectra of CoHNa–beta-III zeolites to Gaussian curves: (a) Co/Al 0.42, component α indicated by a shadow area; (b) Co/Al 0.20, component β indicated by a shadow area; and (c) Co/Al 0.03, component γ indicated by a shadow area.

This strong band was accompanied by a weak band at ca. 21,500 cm^{-1}. Because of the position of the band at 31,500 cm^{-1}, and an increase in its intensity without substantial changes in the d–d transition region, it cannot be related to the d–d transitions; it represents additional Co species exhibiting charge transfer character and is denoted here δ-type Co-species. Some insight into the character of this species was given by changes in the spectra

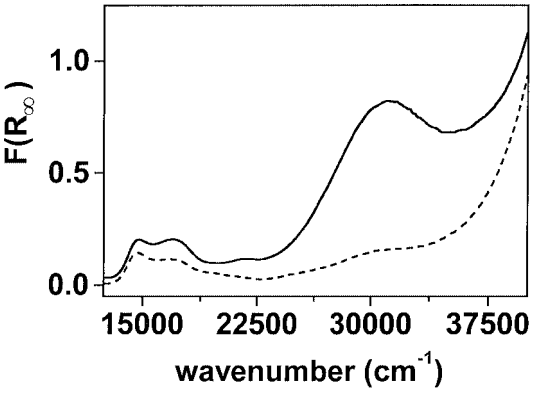

FIG. 3. UV–vis spectra of CoHNa–beta-II: Co/Al 0.35 (- - - -) and 0.42 (——).

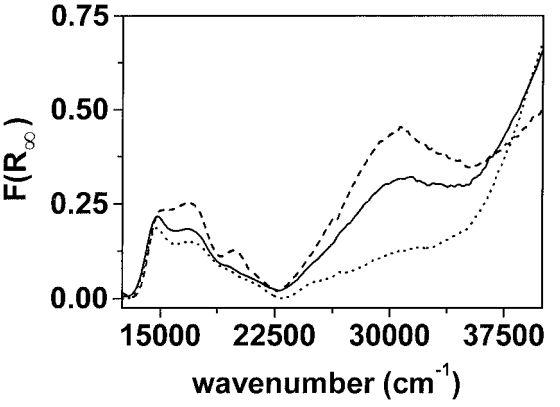

FIG. 4. Dependence of the intensity of the band at 31,500 cm^{-1} on the treatment of Co–beta-II, Co/Al 0.42. Evacuation at 770 K (——), dehydration in an oxygen stream at 720 K (- - - -), and reduction in carbon monoxide stream at 570 K followed by evacuation (· · · ·).

after CoHNa–beta-II (Co/Al 0.42) oxidation and reduction in CO atmosphere (Fig. 4). The intensity of the band at 31,500 cm^{-1} increased after zeolite oxidation with respect to zeolite dehydrated by evacuation. On the other hand, the band intensity dramatically decreased with the zeolite reduced in carbon monoxide. This indicates some oxygen ligands bound to the Co ions with charge transfer character.

Quantitative analysis of the visible spectra: Distribution of Co(II) ions among the individual Co ion types. The resolution of four spectral components, given above, enabled quantitative analysis of the concentration of the individual-type Co(II) ions in dependence on Co/Al and in the presence of Na^+ co-cations to the Co(II) ions, as was described for Co–ferrierite and Co–ZSM-5 zeolites (7, 8). Calculated absorption coefficients are $k_\alpha = 11 \pm 1 \times 10^{-3}$, $k_\beta = 7 \pm 0.7 \times 10^{-3}$, $k_\gamma = 5 \pm 0.5 \times 10^{-3}$, and $k_\delta = 1.3 \pm 0.7 \times 10^{-4}$, $cm \cdot mmol \cdot g^{-1}$. The dependence of the relative concentration of the individual α-, β-, and γ-type Co(II) ions and the δ-type Co ion species in CoHNa–beta-II on Co loading are given in Fig. 5. At low Co content in zeolites all three sites, α, β, and γ, were populated by Co ions in CoHNa–beta-II zeolites, while the δ-type Co species appeared only at high Co loading at Co/Al $\geq$ 0.35. At high Co loading, a relative population of the γ-type Co(II) ions also substantially decreased.

FTIR Spectra of Co–Beta Zeolites

The OH region of the IR spectra of the parent dehydrated beta samples displayed features typical for beta zeolites, with an intensive 3745 cm^{-1} band of terminal SiOH bands, a relatively weak band at 3610 cm^{-1} of the bridged unperturbed OH groups, and a broad band ranging from 3700 to 3400 cm^{-1}, indicating presence of perturbed bridging

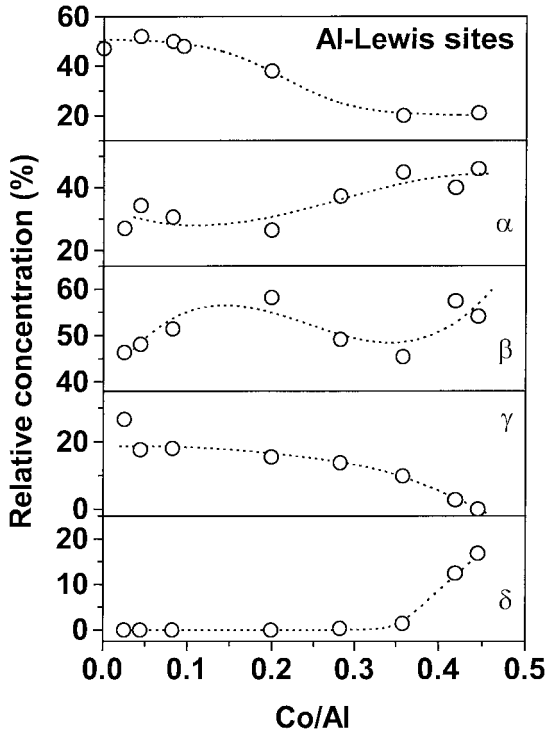

FIG. 5. The effect of the Co loading on the relative concentration of the α-, β-, and γ-type Co(II) ions, on the δ-type Co species, and on the relative concentration of the Lewis sites (within Al-related sites) in CoHNa–beta-II zeolite (concentration of Lewis sites taken from Ref. (6)).

OH groups via hydrogen bonding (not shown in the figure; for more details see Refs. (17–19)). Depending on the conditions of template removal, concentrations of unperturbed and perturbed Brønsted sites varied together with concentrations of Lewis sites (Table 1). More Brønsted sites were present in the beta zeolite when ammonia was present in the stream or when the zeolite contained Na^+ ions in addition to protons. The Lewis sites monitored in parent zeolites were represented by extraframework Al species as well as well as by perturbed Al–O framework bonds exhibiting electron acceptor properties (see 6). As shown previously (6), with an increasing degree of Co(II) ion exchange, at first Na^+ ions were replaced, followed by replacement of sites adjacent to perturbed framework Al–O bonds, and perturbed bridging OH groups. Only a part of the unperturbed OH groups (band at 3610 cm^{-1}) was exchanged by Co(II) ions. Thus the H–beta-I (PQ origin) containing predominantly Lewis sites—extraframework and perturbed framework Al–O bonds (Table 1)—was able to exchange only to a small degree, while with the parent NH_4–beta-IV zeolite exhibiting the highest concentration of Brønsted sites and Lewis sites represented by perturbed Al–O bonds, a high degree of Co exchange was achieved. Nevertheless, with all the beta zeolite samples some unperturbed bridging OH groups remained unchanged, as was reflected in the remaining intensity of the band at 3610 cm^{-1} after Co ion exchange. It follows that the Co(II) ions, and also other cations (including Na^+ or NH_4^+ ions), reconstruct the perturbation of the Al–O framework bonds originally present in parent zeolites, and thus the local framework bonds adjacent to the Co(II) ion. This is a typical feature of beta zeolites, described also in Ref. (6).

IR spectra at the "transmission window" region, i.e., between 1000 and 800 cm^{-1}, are shown in Fig. 6a, and their normalized mode (after Fourier self-deconvolution) on the maximum intensity of the processed bands is given in Fig. 6b. The skeletal bands in this region were assigned to a local perturbation of the zeolite lattice due to bonding of a divalent cation (11–13). For all of the Co–zeolites two bands, i.e., at 901 and 918 cm^{-1}, were indicated. The band at 918 cm^{-1} prevailed with the samples of the Co–beta-I series. The band at 901 cm^{-1} predominated with the Co–beta-II and -IV series at high Co loadings. The samples of Co–beta-IV series exhibited both 901 and 918 cm^{-1} bands of a comparable intensity. Normalized visible spectra corresponding to the FTIR spectra in Figs. 6a and 6b are shown in Fig. 7.

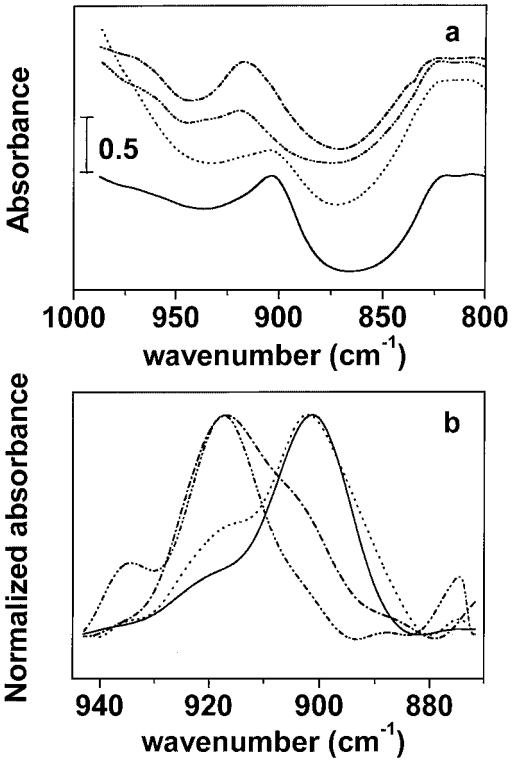

FIG. 6. (a) FTIR spectra in the T–O–T region and (b) normalized FTIR spectra in the T–O–T region of the dehydrated $CoNH_4$–beta-IV (——); CoHNa–beta-II, Co/Al 0.20 (· · · ·); and CoH–beta-I, Co/Al 0.25 (- - - -) and 0.16 (- · - ·).

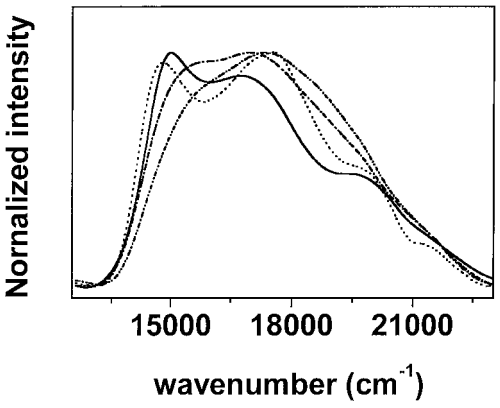

FIG. 7. Visible spectra of the zeolite samples from Fig. 6. $CoNH_4$–beta-IV, Co/Al 0.55 (——); CoHNa–beta-II, Co/Al 0.20 (· · · ·); and CoH–beta-I, Co/Al 0.25 (- - - -) and 0.16 (- · · -).

DISCUSSION

Nature of the α-, β-, and γ-Type Co(II) Ions

The Co(II) spectra in beta zeolites (Fig. 1) can be ascribed to three types of "bare" Co(II) ions (coordinated only to framework oxygens) with different coordination, i.e., at different cationic sites similar to those of the Co(II) ions in dehydrated ferrierite, ZSM-5, and mordenite (7, 8, 10). This is supported by the NIR and by FTIR spectra of dehydrated Co–beta, which show an absence of extraframework ligands in the Co ions. Attribution of the α-, β-, and γ-type Co(II) ions to "bare" ions coordinated at different cationic sites is confirmed by different perturbation of T–O bonds of Co–beta zeolites (Fig. 6, and see below).

Nature of the δ-Type Co Species

In contrast to the α-, β-, and γ-type Co(II) ions characterized by d–d transitions in the visible region, the spectral δ-component in the Co–beta spectrum is characterized by a strong band at 31,500 cm^{-1} (see Figs. 4 and 5). The high energy of this absorption and large width (three times higher in comparison with the maximum band width reported for Co(II) d–d transitions in zeolites (7–10)) indicate a charge transfer (CT) type of electronic transition. This is also supported by the calculated absorption coefficient k_δ ($=1.3 \pm 0.7 \times 10^{-4}$), which is significantly lower (ca. 50 times) than the d–d transitions of the Co(II) ions (note that the extinction coefficient is reciprocal to the absorption coefficient). The extinction coefficients of CT bands are usually 10 to 1000 times higher than extinction coefficients of the d–d bands (20). Thus, the spectral δ-component is suggested to represent oxidiclike Co species. The wavenumber of CT transition of the spectral δ-component (31,500 cm^{-1}) is far from the wavenumbers reported for CT transitions between oxygen and Co(II) (39,000–42,000 cm^{-1}) or Co(III) (27,000 cm^{-1}) ions, according to optical electronegativities given in Ref. (20). However, an absorption band between 31,000 cm^{-1} and 33,100 cm^{-1} is characteristic for bridging μ-superoxo–dicobalt(III) complexes (21–23). Moreover, this strong CT band is usually accompanied by weak bands around 21,000 cm^{-1}. Also in the spectrum of Co–beta zeolites with high intensity of the spectral δ-component, a weak band positioned at 21,500 cm^{-1} is present. The presence of such Co–oxo species might be also supported by the IR band at 2200 cm^{-1} indicated in the spectrum of Co–beta zeolites (not shown in the figures), which is characteristic of the peroxo-vibrations. The Co–Co distance in the $Co–O_2–Co$ complex is 4.5 Å (23). Thus, the distance between the framework oxygens accommodating this μ-oxo–Co complex would be estimated to be ca. 6.5–7.5 Å. This distance fits well with the distance between skeletal oxygen atoms across the beta channels, which displays values from 6.7 to 8.8 Å.

Such μ-oxo–Co species in Co–beta zeolites, observed by Raman spectroscopy, have been reported by Tabata *et al.* (24–26) in Co–beta and ascribed to high and stable activity of Co–beta zeolite in SCR-NO_x in the presence of water vapor.

Cationic Sites of Co(II) Ions in Beta Zeolite

There have not been any suggestions for cation siting in the dehydrated beta structure. However, the similarity in the spectra of the Co(II) ions in dehydrated beta zeolite and in mordenite, ferrierite, and ZSM-5 offers identification of the Co(II) ion sites in beta zeolite. The validity of this approach has been recently confirmed by a synchrotron-powered XRD study of Ni–ferrierite, in which cationic sites in dehydrated ferrierite similar to those suggested from the visible spectra of Co(II) ions have also been identified for Ni(II) ions (27).

In contrast to the other pentasil ring zeolites, such as mordenite, ferrierite, and ZSM-5, the beta zeolite represents a mixture of three polymorphs, A, B, and C (28). Recently pure polymorph C was sythesized (29) and its structure determined (30, 31). Therefore, analysis of the local framework structures related to the characteristic Co(II) d–d transitions can be considered now with respect to these polymorphs.

It was suggested that the α-type Co(II) ions in ferrierite, ZSM-5, and mordenite (7, 8, 10) are coordinated to four framework oxygens of the elongated six-member ring composed of twofold connected five-member rings. The Co(II) ions are supposed to be located above this six-member-ring plane, on top of a pyramid with a base formed by four skeletal oxygens. The location of this site in the beta framework and its local arrangement are depicted in Figs. 8 and 9 (framework structure of polymorph C, according Ref. (31)). Similar local arrangements exist in all three polymorphs of

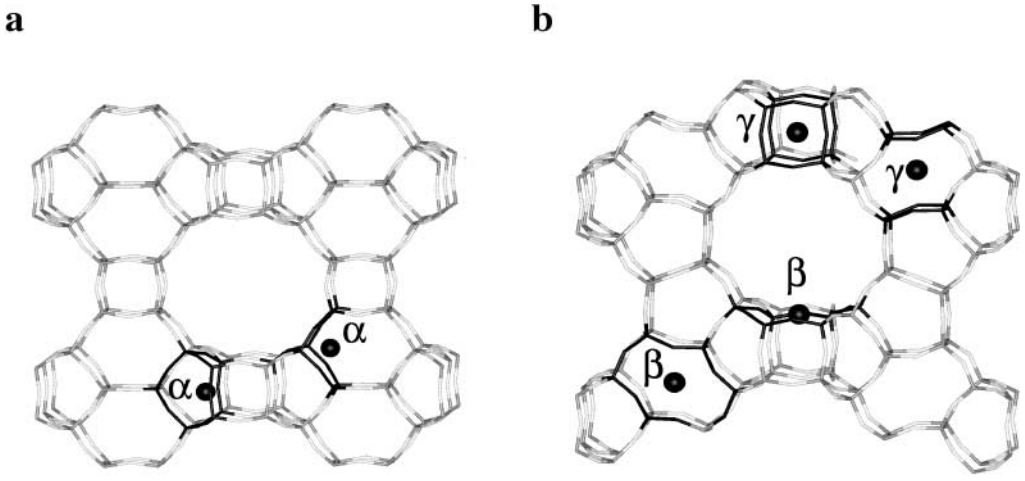

FIG. 8. Location of the α-, β-, and γ-type Co ions in the framework of (a) polymorph C (modeled according to Ref. (31)) and (b) polymorph B (modeled according to Ref. (32)) of beta zeolite.

the beta zeolite. One type of arrangement corresponds to polymorphs A and B, and the second one corresponds to polymorph C. Both of these structures belong to the hexagonal cages of the beta framework (note that local arrangements of these cages is different) and cationic sites are faced inside the cage. However, only the cage in the framework of polymorph C enables Co(II) coordination to four oxygens with the Co(II) ion on top of the pyramid. In polymorphs A and B, another two oxygens are located in the vicinity (ca. 3.3 Å) of the Co(II) ion. Thus, the α-type Co(II) ions, characterized by the single band at 14 600 cm^{-1}, can be attributed to the cationic site formed by an elongated six-member ring composed of twofold five-member rings in the polymorph C of the beta zeolite.

It was suggested the β-type Co(II) ions are coordinated to deformed six-member rings of ferrierite and ZSM-5 or to six oxygens in the plane of a twisted eight-member ring in mordenite (7, 8, 10). These local arrangements result in different distances between framework oxygens and $d_{x^2-y^2}$ and d_{xy} orbitals, and d_{xz} and d_{yz} orbitals of Co(II) ions in all these sites. This is reflected in the quartets of bands in the visible spectra of Co(II) ions. Two different types of simple six-member rings can be found in the beta structures. An elongated six-member ring similar to that of ferrierite is present in beta polymorphs A and B (see Fig. 8b and Refs. (28, 32)). The second type of six-member ring is present in the polymorph C structure. The arrangement of this ring is more regular than that of the rings in polymorphs A and B and three oxygens of this ring are arranged with trigonal symmetry at 2.5 Å away from the ring center. After rearrangement of the ring due to the coordination of the Co(II) ion with a Co–O distance of ca. 2 Å (typical Co–O distance in zeolites, see Ref. (13)), pseudo-trigonal planar symmetry of the Co(II) ion can be supposed. However, trigonal planar coordination of the Co(II) ion is connected with a different Co(II) spectrum, characterized by a band (doublet) around 25,000 cm^{-1} (33). Thus, an elongated six-member ring present in the framework of beta polymorphs A and B is suggested as accommodating β-type Co(II) ions characterized by a quartet of bands, at 15,500, 16,300, 17,570, and 21,700 cm^{-1}. Co(II) ions in this site are accessible from the beta channels. The location of this site in the beta framework (polymorph B) and its local arrangement are depicted in Figs. 8b and 9 (framework structure of polymorph B, according Ref. (32)).

The γ-type Co ions are located in the "boat-shaped" site of mordenite and in similar local arrangements in ferrierite and ZSM-5. Divalent nontransition metal ions in these sites of mordenite and ferrierite are coordinated, according to XRD studies, to six framework oxygens (34) at

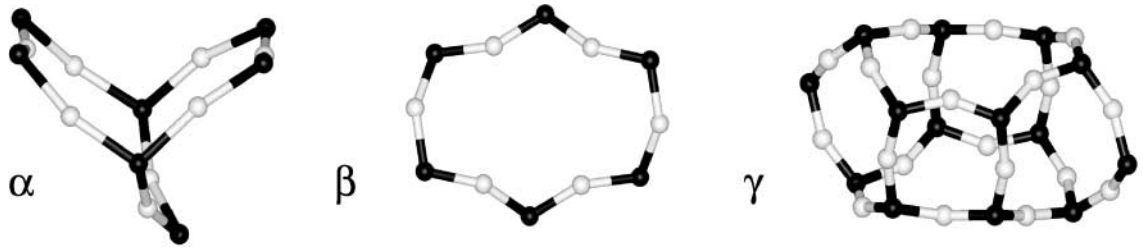

FIG. 9. Local arrangement of α-, β-, and γ-sites in beta zeolites.

approximately octahedral coordination. Thus, a characteristic doublet (18,500 and 20,100 cm^{-1}) of the γ-type Co(II) ions in beta zeolites can be attributed to the closed coordination sphere of the Co(II) ions with octahedral coordination. Although the structure similar to the boat-shaped site is not present in the beta framework, the cations located inside the cage of polymorphs A, B, or C might exhibit symmetry close to the octahedral one. The Co(II) ions located in the cage of polymorphs A and B can occupy a position with deformed bipyramidal symmetry created by six oxygens with a Co(II)–O distance of 2.7–2.85 Å. Inside the cage of polymorph C, Co(II) ions are surrounded by eight framework oxygens at a distance of 2.9–3.05 Å, arranged with deformed cubic symmetry. As the typical Co(II)–O distance in zeolites is ca. 2.0 Å (13, 35), the cage in polymorphs A and B seems to be more appropriate for accommodation of Co(II) ions exhibiting approximately octahedral symmetry. Moreover, α-type Co(II) ions were suggested as occupying a position inside the cage of polymorph C. All other possible sites in beta zeolite enabling formation of a closed coordination sphere are accessible for Co(II) ions only through five- or four-member rings and, thus, are hardly accessible for these ions. Therefore, we suggest that the γ-type Co(II) ions are six coordinated Co(II) ions with approximately octahedral or bipyramidal ligand field symmetry located inside the beta cage of polymorphs A and B. Access to this site from the beta channel system is limited by the size of these six-member rings. The location of this site in the beta framework (polymorph B) and its local arrangement are depicted in Figs. 8b and 9.

In silicon-rich zeolites, distribution of Al atoms represents a key factor in the formation of cationic sites. Only local arrangements of the framework containing two Al atoms represent cationic sites for divalent cations. On the other hand, different positions of the two Al atoms in the same local arrangement cause different cation positions in this local arrangement, which correspond to different cation coordinations necessarily reflected in the different spectra. This was shown for Co(II) ions in the simplest case of a regular six-membered ring (36) or for cation siting in the local arrangement corresponding to the α-site in ferrierite (37). Moreover, in the case of silicon-rich zeolites, occupation of the individual sites at full Co(II) loadings is controlled by the number of cationic sites (from a geometric point of view) containing two Al atoms and does not reflect the steric hindrance known for faujasite or other aluminum-rich zeolites (details in Ref. (8)). Cages in beta zeolite represent complex and large structures (note that cages in polymorphs A/B and C are not identical). Thus, differences in Al distribution in the beta cage can be easy reflected in differences of Co(II) positions. The relation of β- and γ-sites is similar to the relation of sites I'/I in faujasite. In the case of faujasite, both sites can be occupied (but not simultaneously) in the same prism, in contrast to the beta cage (Si/Al $\geq$ 12). Part of cages (containing only one Al atom) do not accommodate Co(II) ions at all, another accommodates Co(II) ions in the β-site (cages with two Al atoms in one six-membered ring), and the last one accommodates Co(II) ions in the γ-site (one Al atom in each opposite six-membered ring). Thus, there is no competition in the space occupation or in balancing of framework negative charge for siting Co(II) ions in β- or γ-sites. The α-site was attributed to the cage in beta polymorph C. This local arrangement is occupied by Co(II) ions when two Al atoms are located in neighboring five-membered rings of this structure. The local arrangement of the A/B cage does not allow such Co(II) coordination (see above). On the other hand, the cage in the C polymorph does not allow coordination of Co(II) ion at the γ-site (see above). Thus, there is no competition for the room or in balancing the framework negative charge between Co(II) ions in the α-site in the beta cage of polymorph C and in the γ-site in the beta cage of polymorphs A/B.

Quantitative Analysis of the Distribution of Co Ions

The absorption coefficients estimated for the α-, β-, and γ-type Co(II) ions in dehydrated Co–beta are of the same order as those found in dehydrated mordenite, ferrierite, and ZSM-5 (7, 8, 10). The differences in the values of the absorption coefficients of the individual Co ions with similar local arrangements in different zeolites can be explained by small differences in their local structure being reflected in slight differences in the band wavelengths corresponding to the individual α-, β-, and γ-type Co(II) ion in zeolites. In contrast, the absorption coefficient of the δ-type Co species in substantially lower, supporting the CT nature of the band at 31,500 cm^{-1}. By using this absorption coefficient, the calculated concentrations of the δ-type Co species are low.

It is necessary to mention that, contrary to other Co–pentasil zeolites (mordenite, ferrierite, and ZSM-5), the dependence of concentration of the α- and β-type Co ions on Co loading does not exhibit monotonic function. On the other hand, it could be hardly attributed to the experimental error (Fig. 5). We can only speculate that this dependence might be affected not only by different preferences in occupation of the cationic sites, but also by replacement of various Al-related sites with the Co(II) ions and by occurrence of polymorphs A, B, and C.

Presence of Co(II) Ions as Reflected in Perturbation of Framework T–O Bonds at Cationic Sites

In accordance with previous results (38), the bands at both 901 and 918 cm^{-1} could be assigned to different Co(II) ions in different cationic sites of beta zeolite. Analogous bands in this region were already found in FTIR spectra of the Co ions bound at cation sites of ferrierite, where they were well correlated with the UV–vis results (13). Similar multiplicity of the bands was also found for the other divalent cations in ferrierite: Mg(II), Mn(II), Ni(II) (11, 33), and Fe(II) (39).

A sequence of spectra of M(II)-ferrierites with increasing concentration of divalent cation revealed a regular pattern, with the band of the highest intensity in a central position of the frequency scale (assigned to the β-site) dominated at all M/Al regions, accompanied by two side bands assigned to the α-site (a band at the higher wavenumber) and γ-site (a band at the lower wavenumber), in agreement with Co(II) visible study (13). This is consistent with the relative position of the T–O–T band, formed due to Co(II) ion bonding in the α- and β-sites in ferrierite, i.e., with the Co spectral α-component at the higher wavenumber providing lower perturbation of the framework bonds.

It is obvious that this picture formed with the Co–ferrierite structure could not be simply adopted to the Co–beta system. The spectral pattern with Co–beta is more complex, and it varies with parent beta zeolites. Obviously, the higher frequency band (α-site) prevails in the CoH–betaA-I, while on $CoNH_4$–beta-IV (parent samples prepared via the NH_3 route) the lower frequency band (β-site) dominates (see Fig. 6), as follows from the UV–vis assignment (see Fig. 7). It implies that the framework α-site is missing in the parent sample containing high concentrations of Lewis sites, presumably both the extraframework Al species and perturbed framework Al–O bonds. On the other hand, the most preserved regular structure of beta zeolite contains high concentrations of framework β-sites, as also occurs in other pentasil ring zeolites (cf. 7, 8, 10). Comparing the results of the UV–vis and IR experiments, the positions of the spectral α- and β-component on the frequency scale, as established in the Co–ferrierite samples, should be actually reversed in the Co–beta system, i.e., the T–O bonds of the α-cationic site are more perturbed compared to that of the β-site. This is in line with the assumption that the framework α-sites are more deformed and easily opened with formation of Lewis sites.

By assuming the established correlation between the position of the α- and β-bands for various M(II) cations in the M(II)–ferrierite samples and the discussion obtained from the model calculation (35), it could be suggested that in the beta zeolites the local perturbation of the framework induced by Co(II) cation at the α-site is higher than that in the β-site. The fact could be taken into consideration that the perturbation as indicated from the DFT calculations (37) consists of several components and the geometric factor could not be necessarily a dominating one. This should be explained by the fact that the α-site corresponds to the polymorph C of the beta framework and that interaction of local structures corresponding to different polymorphs should affect deformation of the site by metal ions coordination.

CONCLUSIONS

Siting of the Co(II) ions in dehydrated Co–beta zeolites is suggested based on the analysis of the visible spectra, the topology of the beta framework, and the parallelism in the visible spectra of the Co(II) ions in beta and mordenite, ferrierite, and ZSM-5. Different Co(II) ion coordination, reflected in characteristic d–d transitions, also induces characteristic perturbations of the T–O framework bonds, reflected in IR skeletal vibrations. The proposed Co(II) ion sites represent the first attempt to describe the siting of divalent metal ions at exchangeable sites of the beta structure, moreover, with consideration of the A, B, and C polymorphs.

Three cationic sites of the Co(II) ions are suggested in the beta zeolite.

- The α-site is formed by an elongated six-member ring composed of a twofold connected five-member rings. This cationic site is present in the framework of the polymorph C of the beta zeolite. The Co(II) ions located at this site are coordinated to four framework oxygens. They are located on top of the pyramid with a base formed by the four oxygen atoms and provide the highest perturbation of the framework T–O bonds. The α-type Co(II) ions are accessible only through six-membered rings of the beta cage and they exhibit a single absorption band at 14,600 cm^{-1} in the vis DR spectra and a band at 901 cm^{-1} in the T–O–T region in FTIR spectra.
- The β-site corresponds to the deformed six-member ring of the hexagonal cage present in polymorphs A and B. The Co(II) ions are located close to the plane of this ring and induce a lower perturbation of the framework bonds at the β cationic site. They are accessible from the beta channel system. The β-type Co(II) ions are characterized by four absorption bands in the visible spectra, at 15,500, 16,300, 17,570, and 21,700 cm^{-1}, and a band at 918 cm^{-1} in the T–O–T region in FTIR spectra. These Co(II) ions predominate in the whole Co loading in all polymorphs of beta zeolites.
- The γ-site is located inside the hexagonal cage present in polymorphs A and B of the beta structure. The Co(II) ions at this site are coordinated to six framework oxygens. They possess a packed coordination sphere, the local arrangement of which is derived from octahedral geometry. These Co(II) ions are accessible through the six-member ring of the beta cage. The γ-type Co(II) ions are reflected in a doublet, at 18,500 and 20,100 cm^{-1}, in visible spectra. They represent a minor concentration of the Co ions in the beta zeolites with high Co loading.

Coordination of the Co(II) ions in cationic sites of beta zeolites is not affected by the original perturbation of the framework Al–O bonds in the parent zeolites, if this perturbation is not so high that it leads to formation of extraframework Al species. Bonding of Co(II) ions at cationic sites with perturbed Al–O bonds reconstruct the Si–O–Al bridges, as this also occurs with the other cations, such as Na^+ or NH_4^+.

On the other hand, the perturbation of the framework T–O bonds in Co–beta due to Co(II) ions at an α cationic site is higher compared to that at the β-site. This is in contradiction to the ZSM-5 and ferrierite zeolites.

The δ-type Co species observed in beta zeolites represent most likely bridging $Co–O_2–Co$ cobalt species. These species are characterized by broad charge transfer (CT) band at 31,500 cm^{-1}. These μ-oxo–cobalt species are formed in the beta zeolite only at the highest Co loading, They represent less than 10% of all the Co ions in the zeolite.

ACKNOWLEDGMENTS

The authors thank Dr. T. Grygar for chemical analysis of the Co–beta zeolites. The research was supported by the Grant Agency of the Czech Republic (Project 104/00/0640) and by the EC COST program via the Ministry of Education, Health, and Sports of the Czech Republic under Project D15-OC15.20.

REFERENCES

1. Ohtsuka, H., Tabata, T., Okada, O., Sabatino, L. M. F., and Bellussi, G., *Catal. Lett.* **44**, 265 (1997).
2. Wichterlová, B., Dědeček, J., and Sobalík, Z., *in* "Catalysis by Unique Metal Ion Structures in Solid Matrices. From Science to Application" (G. Centi, B. Wichterlová, and A. Bell, Eds.), p. 31. Kluwer Academic, Dordrecht, 2001.
3. Li, Y., and Armor, J. N., *J. Chem. Soc. Chem. Commun.* **20**, 2013 (1997).
4. Li, Y., and Armor, J. N., *J. Catal.* **173**, 511 (1998).
5. Wichterlová, B., Dědeček, J., Kaucký, D., and Sobalík, Z., *in* "Proceedings of the 4th European Congress on Catalysis, Rimini, Italy, 1999." Italian Chemical Society, p. 457.
6. Bortnovsky, O., Sobalík, Z., and Wichterlová, B., *Microporous Mesoporous Mater.* **46**, 265 (2001).
7. Kaucký, D., Dědeček, J., and Wichterlová, B., *Microporous Mesoporous Mater.* **31**, 75 (1999).
8. Dědeček, J., Kaucký, D., and Wichterlová, B., *Microporous Mesoporous Mater.* **35–36**, 483 (2000).
9. Wichterlová, B., Dědeček, J., and Sobalík, Z., *in* "Proceedings of the 12th International Zeolite Conference, Baltimore 1998" (M. M. J. Treacy, B. K. Marcus, M. E. Bisher, and J. B. Higgins, Eds.), p. 941. Materials Res. Soc., Warendale, PA, 1999.
10. Dědeček, J., and Wichterlová, B., *J. Phys. Chem. B* **103**, 1462 (1999).
11. Sobalík, Z., Tvarůžková, Z., and Wichterlová, B., *J. Phys. Chem. B* **102**, 1077 (1998).
12. Sobalík, Z., Tvarůžková, Z., and Wichterlová, B., *in* "Proceedings of the 12th International Zeolite Conference, Baltimore, 1998" (M. M. J. Treacy, B. K. Marcus, M. E. Bisher, and J. B. Higgins, Eds.), p. 2339. Materials Res. Soc., Warendale, PA, 1999.
13. Sobalík, Z., Dědeček, J., Wichterlová, B., Kaucký, D., Drozdová, L., and Prins, R., *J. Catal.* **194**, 330 (2000).
14. Rubin, M. K., *U.S. Patent* 5,164,169 (1992).
15. Herzberg, G., "Molecular Spectra and Molecular Structure. II. Infrared and Raman Spectra of Polyatomic Molecules." Van Nostrand, Princeton, NJ, 1945.
16. Wichterlová, B., Tvarůžková, Z., Sobalík, Z., and Sarv, P., *Microporous Mesoporous Mater.* **24**, 223 (1998).
17. Bourgeat-Lami, E., Massiani, P., Di Renzo, F., Espiau, P., and Fajula, F., *Appl. Catal.* **72**, 139 (1991).
18. Kiricsi, I., Flego, C., Pazzuconi, G., Parker, W. O., Jr., Millini, R., Perego, C., and Bellussi, G., *J. Phys. Chem.* **98**, 4627 (1994).
19. Bortnovsky, O., Sobalík, Z., Wichterlová, B., and Bastl, Z., submitted for publication.
20. Lever, A. B. P., "Inorganic Electronic Spectroscopy." Elsevier, Amsterdam, 1984.
21. Miskowski, V. M., Robbins, J. L., Treitel, I. M., and Gray, H. B., *Inorg. Chem.* **14**, 2318 (1975).
22. Lever, A. B. P., and Gray, H. B., *Acc. Chem. Res.* 348 (1978).
23. Miskowski, V. M., Santarsiero, B. D., Schaecher, W. P., Ansok, G. E., and Gray, H. B., *Inorg. Chem.* **23**, 172 (1984).
24. Tabata, T., Ohtsuka, H., Sabatino, L., and Bellussi, G., *Microporous Mesoporous Mater.* **21**, 517 (1998).
25. Tabata, T., and Bellussi, G., *Catal. Today* **42**, 45 (1998).
26. Tabata, T., Ohtsuka, H., Bellussi, G., and Sabatino, L. M. F., *in* "Proceedings of the 12th International Zeolite Conference, Baltimore 1998" (M. M. J. Treacy, B. K. Marcus, M. E. Bisher, and J. B. Higgins, Eds.), p. 1169. Materials Res. Soc., Warendale, PA, 1999.
27. Dalconi, M. C., Cruciani, G., Alberti, A., Ciambelli, P., and Rapacciuolo, M. T., *Microporous Mesoporous Mater.* **39**(3), 423 (2000).
28. http://www.iza-structure.org/databases/.
29. Corma, A., Navarro, M. T., Rey, F., and Valencia, S., *Chem. Commun.* 1486 (2001).
30. Corma, A., Navarro, M. T., Rey, F., Rius, J., and Valencia, S., *Angew. Chem. Int. Ed.* **40**, 2277 (2001).
31. Liu, Z., Ohsuna, T., Terasaki, O., Camblor, M. A., Daz-Lopez, M.-J., and Hirada, K., *J. Am. Chem. Soc.* **123**, 5370 (2001).
32. Newsam, M., Treacy, M. M. J., Koetsier, W. T., and deGruyter, C. B., *Proc. R. Soc. London Ser. A* **420**, 375 (1988).
33. Kellerman, R., and Klier, K., *in* "Surface and Defect Properties in Solids" (M. W. Roberts and J. M. Thomas, Eds.), Vol. 4, p. 1. Chem. Soc., London, 1995.
34. Mortier, W. J., "Compilation of Extra Framework Sites in Zeolites." Butterworth Sci., Guildford, U.K., 1982.
35. Drozdová, L., Prins, R., Dědeček, J., Sobalík, Z., and Wichterlová, B., *J. Phys. Chem. B* **106**, 2240 (2002).
36. Pierloot, K., Delabie, A., Ribbing, C., Verberckmoes, A. A., and Schoonheydt, R. A., *J. Phys. Chem. B* **102**, 10789 (1988).
37. Šponer, J. E., manuscript in preparation.
38. Šponer, J. E., Sobalík, Z., Leszczynski, J., and Wichterlová, B., *J. Phys. Chem. B* **105**, 8285 (2001).
39. Sobalík, Z., Šponer, J. E., Tvarůžková, Z., Vondrová, A., Kuriyavar, S., and Wichterlová, B., *Stud. Surf. Sci. Catal.* **135**, 136 (2001).